

Reaction mechanisms and HCCI combustion processes of mixtures of *n*-heptane and the butanols

Hu Wang^{1,2}, Dan DeVescovo¹, Zunqing Zheng², Mingfa Yao² and Rolf D. Reitz^{1*}

¹ Engine Research Center, University of Wisconsin-Madison, Madison, WI, USA, ² State Key Laboratory of Engines, Tianjin University, Tianjin, China

OPEN ACCESS

Edited by:

Ming Jia,
Dalian University of Technology,
China

Reviewed by:

Derek Splitter,
Oak Ridge National Laboratory,
USA
Francesco Contino,
Vrije Universiteit Brussel,
Belgium

*Correspondence:

Rolf D. Reitz,
Engine Research Center,
University of Wisconsin-Madison,
1500 Engineering Drive,
Madison, WI 53705, USA
reitz@engr.wisc.edu

Specialty section:

This article was submitted to Engine and Automotive Engineering, a section of the journal Frontiers in Mechanical Engineering

Received: 07 February 2015

Paper pending published:

08 March 2015

Accepted: 18 March 2015

Published: 31 March 2015

Citation:

Wang H, DeVescovo D, Zheng Z, Yao M and Reitz RD. (2015) Reaction mechanisms and HCCI combustion processes of mixtures of *n*-heptane and the butanols. *Front. Mech. Eng.* 1:3. doi: 10.3389/fmech.2015.00003

A reduced primary reference fuel (PRF)-alcohol-di-*tert*-butyl peroxide (DTBP) mechanism with 108 species and 435 reactions, including sub-mechanisms of PRF, methanol, ethanol, DTBP, and the four butanol isomers, is proposed for homogeneous charge compression ignition (HCCI) engine combustion simulations of butanol isomers/*n*-heptane mixtures. HCCI experiments fueled with butanol isomer/*n*-heptane mixtures on two different engines are conducted for the validation of proposed mechanism. The mechanism has been validated against shock tube ignition delays, laminar flame speeds, species profiles in premixed flames and engine HCCI combustion data, and good agreements with experimental results are demonstrated under various validation conditions. It is found that although the reactivity of neat *tert*-butanol is the lowest, mixtures of *tert*-butanol/*n*-heptane exhibit the highest reactivity among the butanol isomer/*n*-heptane mixtures if the *n*-heptane blending ratio exceeds 20% (mole). Kinetic analysis shows that the highest C–H bond energy in the *tert*-butanol molecule is partially responsible for this phenomenon. It is also found that the reaction $tC_4H_9OH + CH_3O_2 = tC_4H_9O + CH_3O_2H$ (*tert*-butanol reacts with methylperoxy radical to produce *t*C₄H₉O and methyl peroxide) plays important role and eventually produces the OH radical to promote the ignition and combustion. The proposed mechanism is able to capture HCCI combustion processes of the butanol/*n*-heptane mixtures under different operating conditions. In addition, the trend that *tert*-butanol/*n*-heptane has the highest reactivity is also captured in HCCI combustion simulations. The results indicate that the current mechanism can be used for HCCI engine predictions of PRF and alcohol fuels.

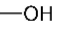
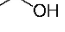
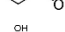
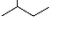
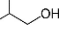
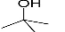
Keywords: HCCI, combustion, butanol isomers, chemical kinetic, mechanism

Introduction

Bio-derived fuels, such as alcohols and bio-diesel, are drawing more and more attention in the internal combustion (IC) engine research community in recent years. Research and applications of these renewable and sustainable biofuels for IC engines and transportation are driven by energy security issues, the increasing dependency on petro-derived diesel/gasoline fuels and also on environment pollutant concerns (Sarathy et al., 2014).

Alcohols have been used as alternative neat fuels or fuel additives in IC engine for years. The major properties of conventional diesel, gasoline, methanol, ethanol, and the four butanol isomers are listed in **Table 1**.

TABLE 1 | Major properties of diesel, gasoline, and alcohols (Sarathy et al., 2014).

	Molecule structure	Molecule weight	Density (kg/m ³)	Research octane number (RON)	T _{boiling} (°C)	Enthalpy of vaporization (kJ/kg from 25°C)	O ₂ (wt. %)	LHV (MJ/kg)
Diesel	C ₁₄ H ₃₀	198.4	802	<0	125–400	351	0	43.4
Gasoline	C ₈ H ₁₅	111.19	720–780	88–98	27–225	232	0	41.2
Methanol		32.04	792	109	64.7	1168	50	19.93
Ethanol		46.06	794	109	78	919.6	35	28.86
<i>n</i> -butanol		74.11	808	98	117.7	707.9	21.62	33.07
<i>s</i> -butanol		74.11	806.3	105	99.5	671.1	21.62	32.90
<i>i</i> -butanol		74.11	788.7	105	108	686.4	21.62	32.96
<i>t</i> -butanol		74.11	801.8	107	82.4	629.9	21.62	32.6

As can be seen, due to the presence of the hydroxyl moiety in the molecule, alcohols are all oxygenated fuels and thus are helpful for soot reduction. The polar structure of the alcohol molecule due to the existence of the hydroxyl moiety also ensures inter-solubility between alcohols and conventional diesel and gasoline fuels, which favors the application of alcohols as fuel additives (Sarathy et al., 2014). The volatilities of alcohols with four carbons and below are higher than diesel, which are important under mixing controlled combustion conditions (Jin et al., 2011). It is found that improvement in volatility by blending alcohols is helpful for soot and CO reduction under low-temperature combustion (LTC) conditions (Wang et al., 2014b). The latent heat of vaporization of alcohols is also significantly higher than those of diesel and gasoline. This can result in difficulties in cold starting when fueling with a high ratio of alcohols. However, the cooling effects of these alcohols can also play a positive role in extending the operation limits in advanced combustion concepts, such as homogeneous charge compression ignition (HCCI) and reactivity controlled compression ignition (RCCI) (Dempsey et al., 2013). In particular, temperature inhomogeneity can be enhanced and compression temperatures can be reduced, which prolong ignition delays and suppress pressure rise rates. The octane number of alcohols is usually close to or even higher than gasoline, which is considerably higher than diesel (Sarathy et al., 2014). Thus, applying alcohols in gasoline spark-ignition (SI) engines is beneficial to suppress the knocking phenomenon. The high octane number of alcohols also favors their application as fuel additives in compression ignition (CI) engine to prolong the ignition delay, promote mixing, and reduce the soot emissions (Zheng et al., 2015).

Methanol and ethanol are currently the most widely used bio-alcohols in IC engine applications. Methanol is mainly produced from coal- or petrol-based fuels while ethanol can be produced by alcoholic fermentation of sugar from vegetable materials, such as corn, sugar cane, and agricultural residues. Ethanol is currently the most widely used biofuel (Jin et al., 2011; Sarathy et al., 2014). Numerous fundamental investigations on these alcohols can be found, including kinetic oxidation mechanisms (Marinov, 1999; Li et al., 2007; Metcalfe et al., 2013), shock tube ignition delays (Heufer and Olivier, 2010; Noorani et al., 2010; Kumar and Sung, 2011), laminar flame speeds (Zhang et al., 2008; Veloo et al., 2010; Beeckmann et al., 2014), flow reactors

(Norton and Dryer, 1991; Esarte et al., 2012; Aranda et al., 2013), premixed flames (Veloo et al., 2010; Leplat et al., 2011; Xu et al., 2011), and jet-stirred reactors (JSR) (Dayma et al., 2007; Dagaut and Togbé, 2010; Leplat et al., 2011). In addition to fundamental studies, these alcohols have also been widely applied as neat fuels or additives to improve the performance and emissions of both CI and SI engines (Agarwal, 2007; Elik et al., 2011; Canakci et al., 2013; Balki et al., 2014). Canakci et al. (2013) found that blending methanol and ethanol with gasoline in SI engine could be helpful for reducing carbon dioxide (CO₂), unburned hydrogen carbon (UHC), and NO_x emissions. Rakopoulos et al. (2008) showed that mixtures of ethanol and diesel can significantly reduce the soot emission, and a slight reduction in CO and NO_x can also be obtained. Agarwal (2007) concluded that applying ethanol as a gasoline additive could significantly reduce CO and UHC at all engine speeds in SI engines. In addition, up to 20% of ethanol can be blended with diesel to be used in CI engines without any hardware modification (Ajav et al., 1999). In addition, reduction in soot, CO, and NO_x emissions can be achieved and cold-start performance is not affected.

In addition to methanol and ethanol, butanol has also drawn increasing attention in recent years. Butanol has four carbon atoms and thus four isomers exist depending on the position of the OH radical in the molecule. The molecular structures and properties of the four isomers are also listed in **Table 1**. Like ethanol, butanol is also a renewable and sustainable biofuel, which can be produced by alcoholic fermentation of biomass feedstocks (Jin et al., 2011). It is seen in **Table 1** that due to the increased number of carbon atom in the molecule, the reactivity of butanol is slightly higher than methanol and ethanol (RON 98~107 versus 109), but the latent heat of vaporization of butanol is much lower than methanol and ethanol, which indicates that cold-start performance in CI engines fueled with butanol can be improved compared to methanol and ethanol. The oxygen content decreases as the number of carbon atoms increases in the molecule, thus the oxygen content in the butanol isomers is considerably lower than methanol and ethanol. *n*-butanol has been applied as a fuel additive in both CI and SI engines by many researchers (Rakopoulos et al., 2010; Yao et al., 2010; Gu et al., 2012; Chen et al., 2014; Liu et al., 2014; Wang et al., 2014b). *Iso*-butanol is also becoming an attractive fuel since its physical properties are very

close to *n*-butanol, but with higher auto ignition resistance. This actually favors its application in dual-fuel RCCI combustion to serve as the premixed low reactivity fuel. The general conclusion is that soot emissions can be greatly reduced, while the combustion and thermal efficiency are comparable to neat diesel in CI engines, with additional benefits in CO and UHC reduction. Gu et al. (2012) found that blends of gasoline and *n*-butanol decrease engine specific UHC, CO, and NO_x emissions compared to those of gasoline, and that particle number concentrations can also be reduced with gasoline and *n*-butanol mixtures.

Therefore, fundamental investigations related to butanol isomers are currently of interest in the IC engine research community. Moss et al. (2008) proposed a kinetic mechanism for the high temperature oxidation of the four butanol isomers to predict ignition delays measured in shock tube. Dagaut et al. (2009) and Dagaut and Togbe (2009) studied the oxidation of neat *n*-butanol and mixtures of *n*-butanol and *n*-heptane in a JSR, and a kinetic mechanism for *n*-butanol was proposed. Sarathy et al. (2009), Black et al. (2010), Harper et al. (2011), and Heufer et al. (2011) also studied *n*-butanol oxidation processes through both experimental and kinetic investigations in shock tube, JSR, and counter flow flames. However, these studies mainly focused on the high temperature oxidation process, and no low-temperature reaction pathway was proposed and included in these mechanisms. Vranckx et al. (2011) studied the role of peroxy chemistry in the high-pressure ignition of *n*-butanol. A low-temperature reaction pathway for *n*-butanol was proposed, which was based on the *n*-heptane low-temperature branching reaction pathway. Ignition delays from shock tubes between 795 and 1200 K were taken to validate the proposed mechanism. Negative temperature coefficient (NTC) behavior was observed in the *n*-butanol oxidation process. Low-temperature reaction pathways for *iso*-butanol and *tert*-butanol were also studied by Welz et al. (2013). Sarathy et al. (2012) proposed a detailed chemical kinetic mechanism for the oxidation of the butanol isomers, which includes the complete high-temperature and low-temperature reaction pathways for all isomers. Ignition delays from shock tube and rapid compression machine (RCM), laminar flame speeds, and species profiles from premixed flat flames and JSRs were taken to validate the mechanism. In addition to these kinetic studies, shock tube and RCM ignition delays (Weber and Sung, 2013; Yang et al., 2013; Bec et al., 2014; Pan et al., 2014), laminar flame speeds (Velloo and Egolfopoulos, 2011; Wu and Law, 2013), species profiles from JSR, premixed flames (Dagaut et al., 2009; Togbé et al., 2010; Oßwald et al., 2011; Welz et al., 2013) can also be found in the literature.

Many advanced algorithms have been developed to improve the computational efficiency of computational fluid dynamic (CFD) simulations coupled with detailed kinetic mechanisms. For example, Perini et al. (2012, 2014) developed an analytical Jacobian approach for sparse reaction kinetics to improve the computational efficiency of large reaction mechanisms, and up to three orders of magnitudes speed-up were achieved by using this “SpeedCHEM” solver. Shi et al. (2011) utilized the graphics processing unit (GPU) for combustion modeling, and one order of magnitude acceleration was obtained. However, even with the help of these advanced algorithms and hardware, detailed

mechanisms are still too large to be applied for engine combustion simulations.

With the aim of applying butanol kinetic mechanisms for engine CFD simulations, detailed mechanisms must be reduced to a reasonable size to improve computational efficiency. Currently, very few reduced butanol mechanisms are available from the literature for engine combustion simulations. Liu et al. (2011) proposed a reduced *n*-butanol mechanism with 66 species based on Dagaut et al.’s mechanism (Dagaut et al., 2009). However, even the base mechanism did not include the low-temperature reactions for *n*-butanol, which is crucial for engine combustion simulations. Wang et al. (2013a) proposed a reduced *n*-heptane/*n*-butanol/PAH mechanism and validated the mechanism against available shock tube ignition delays, *n*-heptane/*n*-butanol engine HCCI, and direct injection compression ignition (DICI) combustion data. The proposed mechanism was also used to investigate the effects of *n*-butanol oxygenated fuel on soot formation processes.

The objective of the current study is to develop an integrated reduced primary reference fuel (PRF)–methanol–ethanol–butanol–di-*tert*-butyl peroxide (DTBP) mechanism for engine combustion simulations. Such mechanism makes it possible to model HCCI, RCCI, DICI, and SI engine combustion with both conventional gasoline and diesel fuels and alternative alcohols. The detailed butanol mechanism developed by Sarathy et al. (2012) is taken as the baseline mechanism, and mechanism reductions for the four butanol isomers are conducted and are then integrated into a base-reduced PRF mechanism. The mechanism has been validated with available experimental data including shock tube ignition delays, laminar flame speeds, and species profiles from premixed flames. HCCI combustion data for the mixtures of *n*-heptane and the butanol isomers are also collected to validate the performance of the proposed mechanism on two different diesel engines. The paper starts with the mechanism formulation, followed by details of mechanism adjustment and validation, and finally experimental and simulation results for HCCI combustion processes of *n*-heptane/butanol mixtures are presented and discussed.

Mechanism Formulation

Base-Reduced PRF Mechanism

The reduced PRF–methanol–ethanol–DTBP mechanism developed by Wang et al. (2013b); Wang et al. (2014a) was taken as the base mechanism. This reduced PRF mechanism was constructed hierarchically, from the core H₂–C₁–C₂ sub-mechanism, then the C₃ intermediate mechanism and finally the simplified reaction pathways for *n*-heptane and *iso*-octane from C₇–C₈ to C₃ species. The core mechanism was taken from the detailed C₁–C₂ mechanism developed by Metcalfe et al. (2013) (Aramco Mech 1.3). The methanol and ethanol sub-mechanisms were also included in this core mechanism. A reduced DTBP kinetic mechanism was constructed based on available literature mechanisms and it was incorporated into the base mechanism. This sub-mechanism was considered in the reduced mechanism to characterize the reactivity enhancement effects of DTBP to methanol and

ethanol. The most important intermediate species during DTBP oxidation, $t\text{-C}_4\text{H}_9\text{O}$, which arises through the decomposition reaction $\text{DTBP} = 2t\text{-C}_4\text{H}_9\text{O}$, is also an important intermediate species for $t\text{-C}_4\text{H}_9\text{OH}$ oxidation. Therefore, the DTBP sub-mechanism is also included in the current mechanism. In Wang et al.'s study (Wang et al., 2014a), a detailed C_1 core mechanism was required to reproduce the reactivity enhancement effect of DTBP with methanol and ethanol, thus the prediction capability of the core mechanism is assured. This base-reduced mechanism has been extensively validated with various experimental data, including ignition delays, laminar flame speeds, species profiles from flames, and combustion data from HCCI, premixed charge compression ignition (PCCI), RCCI, and DICI engines. Details about the base mechanism can be found in Wang et al. (2013b, 2014a).

Butanol Mechanism

The detailed oxidation mechanism for the four butanol isomers developed by Sarathy et al. (2012) was taken as the parent mechanism for the mechanism reduction. This detailed mechanism contains both low-temperature and high-temperature reaction pathways for all butanol isomers and has been extensively validated with available experimental data. Since the core C_2 mechanism and intermediate C_3 mechanism show reliable performance under various validation conditions, the present reduced butanol sub-mechanisms were constructed by formulating simplified reaction pathways from the butanol molecule to the species that already exist in the base PRF mechanism. In other words, the butanol sub-mechanisms are treated as modules, which can be assembled with the base PRF mechanism to formulate more generic mechanisms. Direct relation graph with error propagation (DRGEP) (Pepiot-Desjardins and Pitsch, 2008; Shi et al., 2010), reaction pathway, rate of production, and sensitivity analyses were used for the mechanism reduction. In the reduction process, the ignition delay and laminar flame speed were chosen as the targets and were validated against either the detailed mechanism or experimental data after each reduction step Wang et al. (2013b, 2014a).

Table 2 shows the major steps involved in the reaction pathways for the butanol isomers. It is seen that the structures of the reduced mechanisms are similar to the typical alkane oxidation mechanism, which contain the complete low-temperature and high-temperature reaction pathways. The low-temperature branching reactions, listed from step-4 to step-8 in Table 2, are mostly retained for the butanols. In order to keep the reduced mechanisms as small as possible to improve computational efficiency, only one H atom abstraction product was kept for each isomer except n -butanol, for which was found that the laminar

flame speed highly depends on reactions involving $n\text{-C}_4\text{H}_8\text{OH-1}$ and $n\text{-C}_4\text{H}_8\text{OH-3}$. Thus, reactions related to these two species were kept in the reduced n -butanol sub-mechanism. Due to the fact that very limited experimental ignition delay data are available for mechanism validation under engine-like conditions during the mechanism reduction, the prediction results from the detailed parent mechanism were taken to serve as the target.

Mechanism Formulation

After mechanism reduction, the reduced butanol isomer sub-mechanisms were incorporated into the base PRF-methanol-ethanol-DTBP mechanism to formulate an integrated reduced PRF-alcohol-DTBP mechanism. Only 5–7 species and 14–21 reactions from each butanol sub-mechanism were required to be incorporated into the base PRF mechanism. This results in an integrated PRF-alcohol mechanism with 108 species and 435 reactions. The integrated mechanism contains oxidation mechanisms for the following fuels: n -heptane, iso -octane, methanol, ethanol, DTBP, and the four butanol isomers. The thermodynamic and transport properties for all the species in the reduced butanol mechanisms were taken from the detailed parent mechanism of Sarathy et al. (2012).

Mechanism Adjustment

Due to the different core mechanisms between the detailed butanol and reduced PRF mechanisms, some adjustment and optimization were required to improve the prediction accuracy of the integrated mechanism. It has been pointed out that even if a standalone mechanism performs well, this does not ensure that the combined mechanism also can accurately predict the ignition and combustion characteristics of fuel mixtures. The interactions between different sub-mechanisms in the integrated mechanism can greatly affect the overall performance of a mechanism.

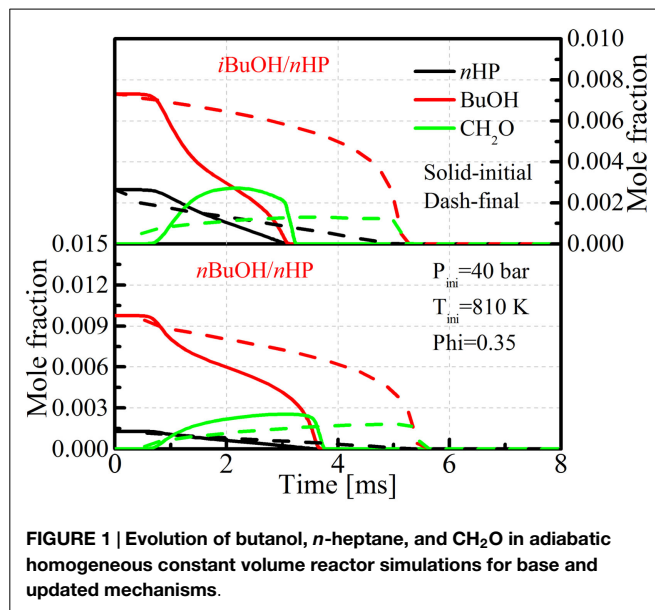
In the current study, similar issues were seen after simply combining the sub-mechanisms to formulate the integrated mechanism. The prediction capabilities of the integrated mechanism for the neat fuels, such as n -heptane and the butanol isomers, were almost identical to their, respectively, standalone mechanisms. However, the performance of the integrated mechanism in butanol-heptane HCCI combustion simulations deviated from the experimental results, which motivated the above-mentioned concerns.

It is known that butanol is a forceful competitor for the OH radical formed from n -heptane, and the OH radical produced from high reactivity n -heptane is consumed by alcohol components. This retards the ignition delay compared to neat n -heptane (Karwat et al., 2012; Zhang et al., 2013). As a result, the consumption rate of n -heptane is reduced while the oxidation rate of butanol is enhanced. Zhang et al. (2013) found that during the oxidation of n -butanol/ n -heptane mixtures the consumption of n -heptane was inhibited while that of n -butanol was enhanced since their competition for OH radicals is mainly produced in the low-temperature reaction stage of n -heptane.

Figure 1 shows evolution processes of n -heptane/butanol mixtures in adiabatic homogeneous constant volume reactor simulations, wherein a representative condition prior to ignition from n -butanol/ n -heptane HCCI combustion (see HCCI Combustion below) is taken as the initial condition for simulation, performed

TABLE 2 | Major reaction pathways in the reduced butanol isomer mechanisms.

Step-1	Unimolecular fuel decomposition
Step-2	H atom abstraction (OH, HO ₂ , O ₂ , O, CH ₃ O ₂)
Step-3	Fuel radical decomposition
Step-4	Addition of O ₂ to fuel radicals
Step-5	ROO radical isomerization
Step-6	Addition of O ₂ to QOOH
Step-7	O ₂ QOOH = keto-hydroperoxide + OH
Step-8	Keto-hydroperoxide decomposition



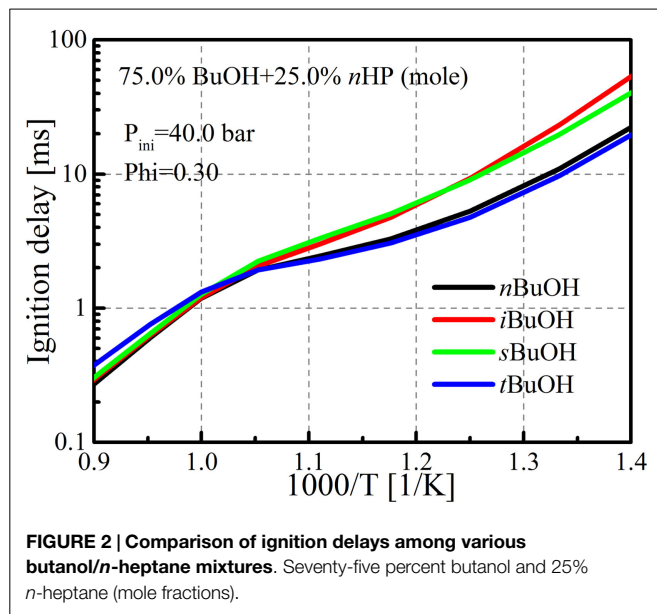
with the Reaction Design (2008). The solid lines in **Figure 1** indicate the base-integrated mechanism without any adjustments. It is seen that the consumption rates of both *n*-butanol and *iso*-butanol are actually faster than *n*-heptane and show two-stage oxidation processes. The mostly possible reason for this phenomenon is that the reaction rate of butanol + OH is too fast, and that most of the OH radicals generated from the *n*-heptane low-temperature branching reactions are stolen to take part in butanol + OH reactions.

Haas et al. (2011) measured the relative reactivity of mixtures of butanol and *n*-heptane in an ignition quality tester (IQT), and it was found that the reactivity of butanol/*n*-heptane mixtures does not agree with their research octane number (RON) or cetane number (CN) when a single neat fuel was used. Specifically, it was found that although the neat *n*-butanol has the highest reactivity, followed by *sec*-butanol and *iso*-butanol, and *tert*-butanol has the lowest reactivity, which has been proved by many kinetic studies (Sarathy et al., 2012; Stranic et al., 2012; Bec et al., 2014). However, mixtures of *tert*-butanol and *n*-heptane exhibit the highest reactivity (highest CN) compared to the other three-butanol isomers. The different C–H bond energy in the molecule was used to explain the phenomenon. The lowest C–H bond energy in the *n*-heptane molecule is around 98.6 kcal/mol (Hudzik et al., 2014), while the lowest C–H bond energies in *n*-butanol, *sec*-butanol, and *iso*-butanol are close, about 95 kcal/mol. However, *tert*-butanol has the highest C–H bond energy among these fuels (103.9 kcal/mol) (Sarathy et al., 2012). In the mixtures of butanol and *n*-heptane, the most reactive OH radical produced through the *n*-heptane low-temperature branching reaction is the key factor that affects the overall reactivity. Butanol and *n*-heptane compete with each other for the OH radical. Due to the lower bond energies in *n*-butanol, *iso*-butanol, and *sec*-butanol, theoretically the reaction rate of H atom abstraction through the OH radical for these three butanol isomers should be higher than *tert*-butanol. Therefore, *n*-butanol, *iso*-butanol, and *sec*-butanol

actually serve as OH *sinks* in this process, which reduces the amount of available reactive OH radical that can participate in the *n*-heptane low-temperature branching reaction, thus greatly reduces the overall reactivity. However, since the *tert*-butanol molecule has the highest C–H bond energy, the reaction rate of H atom abstraction through OH is considerably lower than for the other three isomers and *n*-heptane. Therefore, OH radicals generated from *n*-heptane have a higher tendency to be involved in low-temperature reaction pathways, which further promote the production of OH radicals, and result in the highest reactivity for *tert*-butanol/*n*-heptane mixtures.

Therefore, the H atom abstraction reaction rates through OH for the four butanol isomers were adjusted to follow above analysis. The reaction constants of several other reactions in the reduced butanol mechanisms were also adjusted to match ignition delays predicted by the detailed mechanism and experimental results. Since the base PRF mechanism has been extensively validated with various experimental data, it was kept intact.

However, it was found that these optimizations were still not sufficient to reproduce the highest reactivity behavior of *tert*-butanol/*n*-heptane mixtures in HCCI combustion. Sensitivity analysis was then conducted for *tert*-butanol/*n*-heptane mixtures to identify the reactions that are important to the reactivity. It was found that the reaction $t\text{C}_4\text{H}_9\text{OH} + \text{CH}_3\text{O}_2 \rightleftharpoons t\text{C}_4\text{H}_9\text{O} + \text{CH}_3\text{O}_2\text{H}$ (*tert*-butanol and methylperoxy radical \rightleftharpoons *tert*-butanol and methyl peroxide) plays an important role in determining the mixture's reactivity. This reaction is important due to the fact that *t*C₄H₉O undergoes the following reactions: $t\text{C}_4\text{H}_9\text{O} \rightarrow \text{CH}_3\text{COCH}_3$ (acetone) + CH₃ (methyl radical) \rightarrow CH₃O₂ (methylperoxy radical) \rightarrow CH₃O₂H (methyl peroxide) \rightarrow CH₃O (methoxy radical) + OH (hydroxyl radical), which eventually produces additional OH radicals to promote the ignition. This is also the most important pathway in the DTBP oxidation mechanism, since the DTBP molecule quickly decomposes into two *t*C₄H₉O radicals, which was found to be partially responsible for the reactivity enhancement of DTBP to serve as a cetane improver (Wang et al., 2014a). Therefore, the reaction rate of $t\text{C}_4\text{H}_9\text{OH} + \text{CH}_3\text{O}_2$ (methylperoxy radical) \rightleftharpoons $t\text{C}_4\text{H}_9\text{O} + \text{CH}_3\text{O}_2\text{H}$ (methyl peroxide) was increased and the reaction constants for other reactions, mainly the $t\text{C}_4\text{H}_9\text{OH} + \text{HO}_2 \rightleftharpoons t\text{C}_4\text{H}_9\text{O} + \text{H}_2\text{O}_2$ were also adjusted to match the ignition delays predicted by the detailed mechanism. The evolution processes of the fuels and CH₂O with the updated mechanism are also shown in **Figure 1**. It is seen that the consumption and oxidation processes are more reasonable, and that fast consumption of butanol only occurs after a long ignition preparation stage. **Figure 2** shows comparisons of ignition delays for mixtures of the butanol isomers and *n*-heptane under the adiabatic homogeneous constant volume condition. The mixtures consist of 75% (mole) butanol and 25% *n*-heptane (mole), and the pressure and equivalence ratio are 40.0 bar and 0.3, respectively, which are very close to the operating condition in the butanol/*n*-heptane HCCI engine experiments, which will be presented in the Section "HCCI Combustion." It is seen that the mechanism is capable of capturing the reactivity trend among the butanol isomers. The mixture *tert*-butanol/*n*-heptane shows the highest reactivity, followed by *n*-butanol, which is



close to *tert*-butanol, and the ignition delays of *sec*-butanol/*n*-heptane and *iso*-butanol/*n*-heptane mixtures are much longer than *tert*-butanol and *n*-butanol, which agrees with the results found by Zheng et al. (2015) and Haas et al. (2011), and also the HCCI combustion results of the current study. The complete mechanism is provided as Supplementary Material and can be downloaded from the Engine Research Center (2013).

Mechanism Validation

Validations of the base PRF mechanism have been extensively discussed in the authors' previous works, and thus are not presented here. Details about the mechanism can be found in Wang et al. (2013b, 2014a).

Ignition Delay

Limited experimental ignition delays are available for the validation of butanol mechanisms, especially under low-temperature conditions (700–1000 K), which is very important for advanced combustion concept simulations. Therefore, the ignition delays predicted by the parent detailed mechanism were taken to validate the reduced mechanism. **Figure 3** shows comparisons of the ignition delays predicted by the detailed and current reduced mechanisms under two equivalence ratio conditions at an initial pressure of 40.0 bar. The simulations were conducted with the Reaction Design (2008) and ignition delay is defined as the time of maximum (dT/dt). It is seen in **Figure 4** that the ignition delays predicted by the current reduced mechanism agree quite well with the detailed mechanism for the four butanol isomers under different conditions.

In addition to the comparisons between mechanism predictions, the experimental ignition delays measured by Stranic et al. (2012) (temperature 1050–1600 K, pressure 17–48 bar, equivalence ratio 0.5 and 1.0), Heufer et al. (2011) (temperature 770–1250 K, pressure 10–42 bar, equivalence ratio = 1.0), Vranckx

et al. (2011) (*n*-butanol, temperature 795–1200 K, pressure 61–92 bar, equivalence ratio = 1.0), Zhu et al. (2013) (constrained-reaction-volume (CRV) strategy to measure the ignition delay of *n*-butanol, temperature 716–1121 K, pressure 20–40 bar, equivalence ratio = 0.5, 1.0, and 2.0), and Bec et al. (2014) (CRV) strategy for *sec*-, *iso*-, and *tert*-butanol, temperature 828–1095 K, pressure 20–30 bar, equivalence ratio 0.5 and 1.0) were also taken to validate the proposed mechanism. **Figure 4** shows ignition delay comparisons between simulations and experiments for the butanol isomers. It is seen that the current reduced mechanism provides reasonably good predictions for all the butanol isomers under different conditions. The relative differences among the butanols are well captured by the mechanism. For the neat butanols, *tert*-butanol shows the longest ignition, *n*-butanol shows the shortest ignition delay, while the other two are between these two isomers.

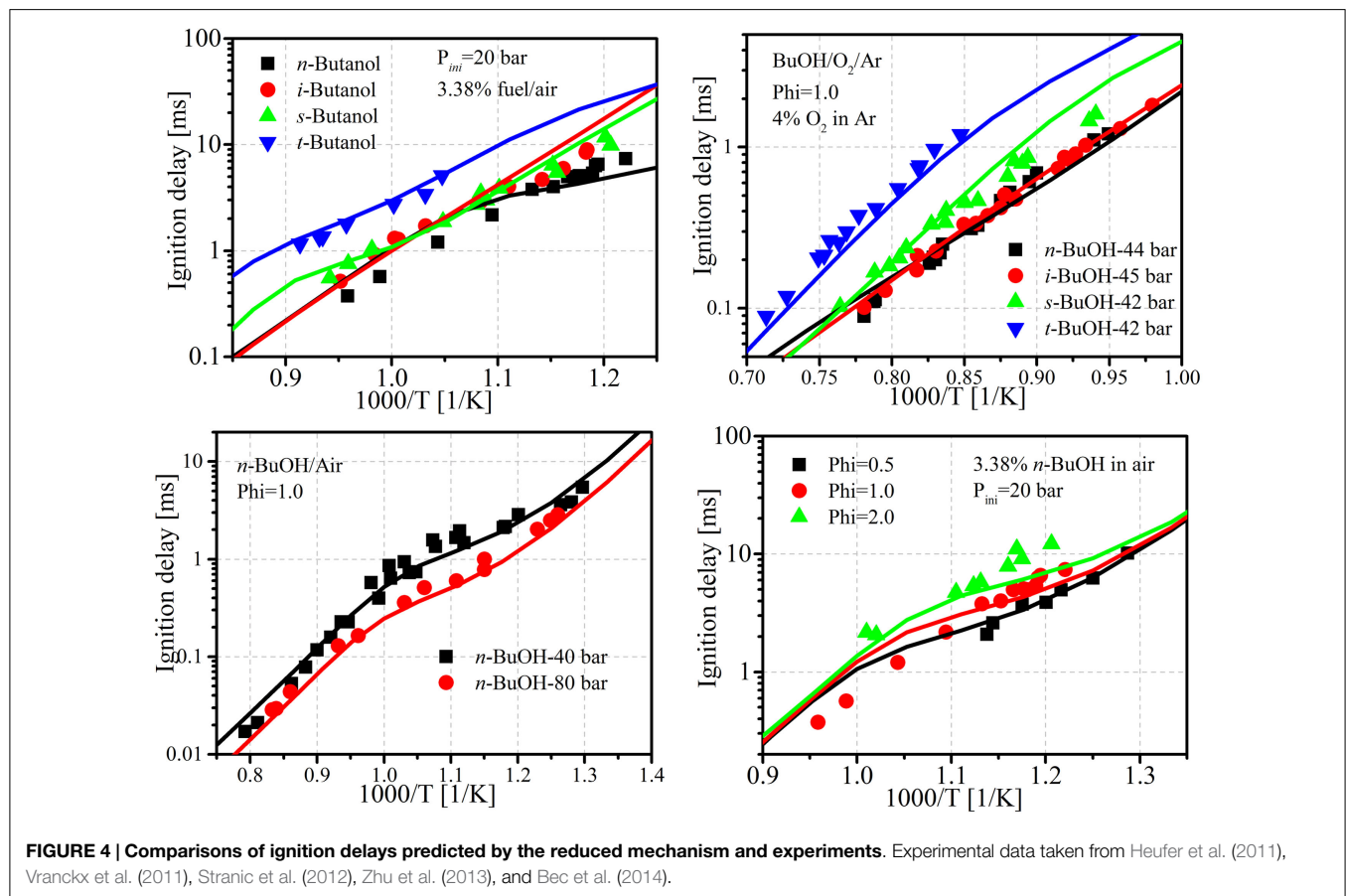
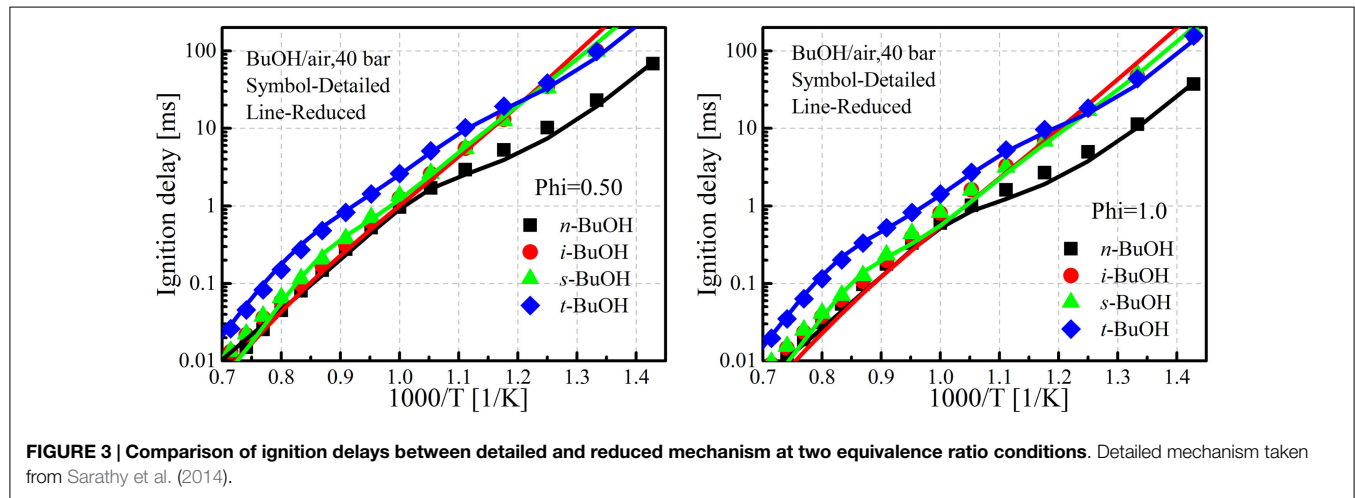
Additional low-temperature ignition delay validations for neat *n*-butanol are also shown in **Figure 4**, and good agreements are obtained with the current reduced mechanism. Although there are other available experimental data for the validation of *n*-butanol/*n*-heptane mixtures, they are all under high temperature and low-pressure conditions, such as the works of Karwat et al. (2012) and Zhang et al. (2013), and are thus not included in the current study.

Laminar Flame Speeds

Figure 5 shows comparisons of laminar flame speeds between the predictions of the current mechanism and experimental results from Veloo and Egolfopoulos (2011) and Wu and Law (2013). Veloo and Egolfopoulos (2011) measured the flame propagation of four butanol isomers in counter flow flames under atmospheric pressure and an unburned mixture temperature of 343 K. Wu and Law (2013) also measured the laminar flame speeds for four butanol isomers in a heated, dual-chamber vessel at pressure 1–5 bar, and unburned temperature of 353 and 373 K. The uncertainty of the measurements was estimated to be within 2.0 cm/s. The simulations were conducted with the Reaction Design (2008). It is seen that satisfactory agreements between the simulations and experiments are obtained with the current reduced mechanism. The relative differences among the butanol isomers are also captured by the proposed mechanism.

Species Profiles in Premixed Flame

Oßwald et al. (2011) conducted a detailed molecular beam mass spectrometry (MBMS) investigation of the four butanol isomer's flame chemistry in flat, premixed, laminar low-pressure (40 mbar) flames. Fuel-rich (equivalence ratio = 1.7) butanol/oxygen/25% argon flames were investigated using different MBMS techniques and the measurements were taken to validate the present mechanism. The uncertainty of the measurements may be as low as 20%, depending on the detected species, but can reach up to two to four times difference with the estimation of the cross sections. The flames consisted of 16.5% butanol/58.1% O₂/25.4% Ar (mole fraction) under ambient pressure of 4 kPa and an inlet flow rate of 32.3 cm/s. Details about the experimental setup can be found in Oßwald et al. (2011). **Figure 6** shows the predictions of the major reactants and products with the reduced mechanism. It is seen that the overall agreements are reasonably good for all isomers.

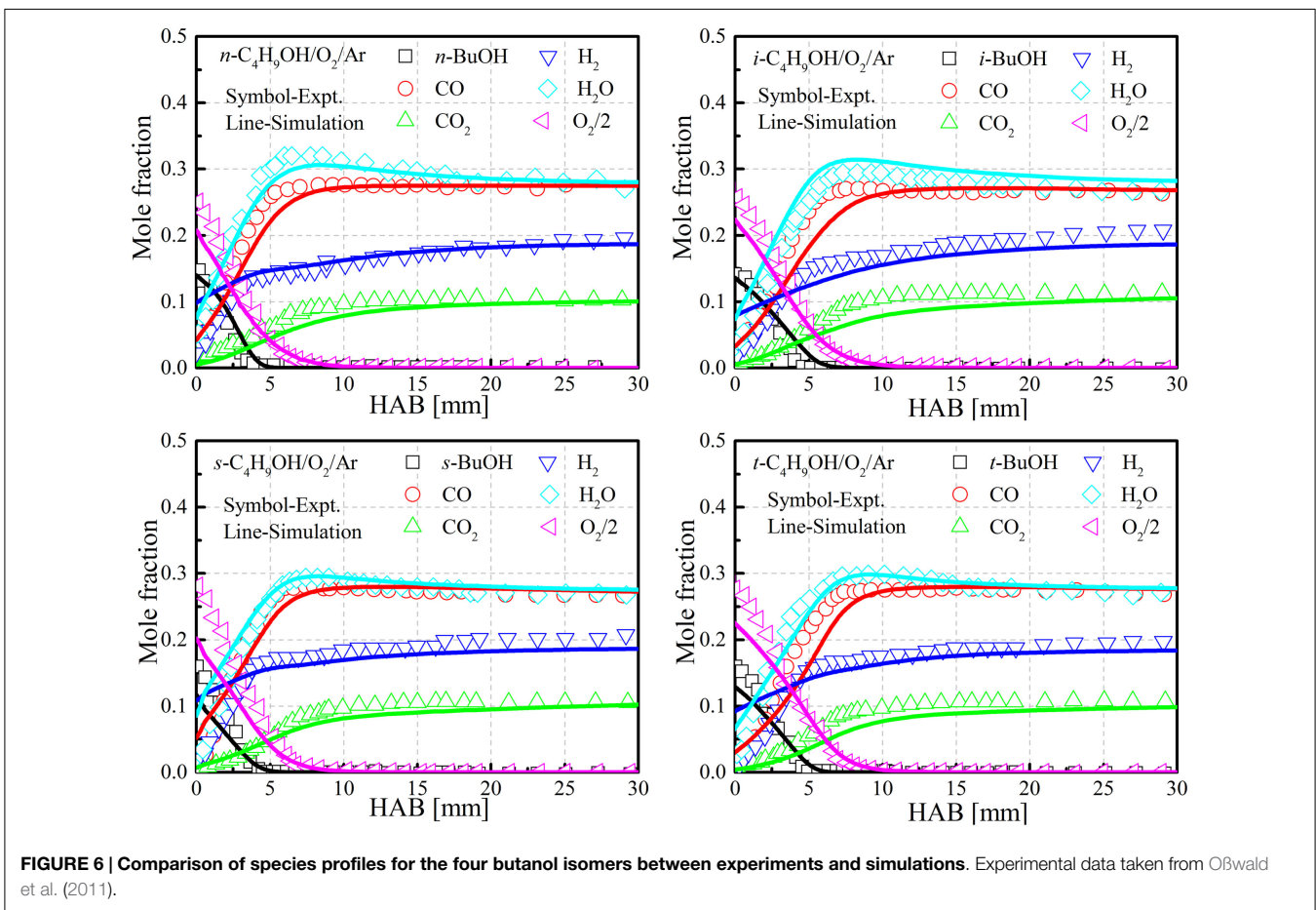
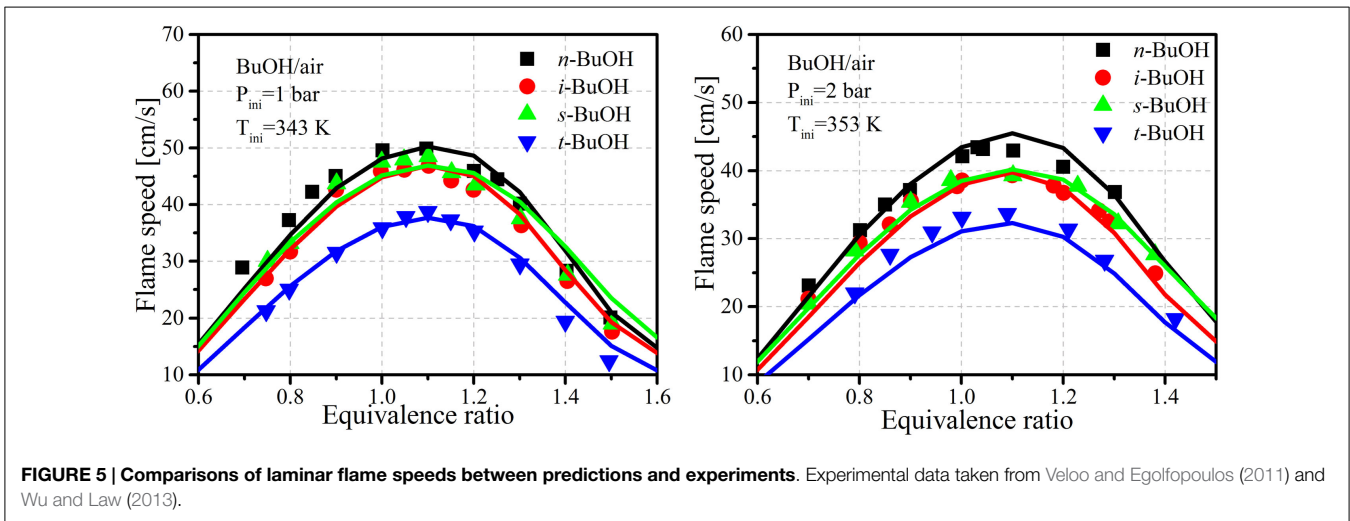


HCCI Combustion

In the current study, HCCI combustion processes of butanol/*n*-heptane mixtures were also conducted to further validate the proposed mechanism. Mixtures of butanol/*n*-heptane were chosen due to the fact that the reactivity of butanol, even the isomer with the highest reactivity, *n*-butanol, still has a RON of 93, for which it is difficult to achieve stable HCCI combustion without intake heating. Thus *n*-heptane was blended with the butanol isomers

to improve the fuel reactivity. HCCI experiments were conducted on two different engines. The engine specifications and operating conditions for the HCCI operation are listed in **Table 3**.

In the CAT (Caterpillar) SCOTE engine, a piston with compression ratio (CR) of 14.88 was used and mixtures of two butanol isomers (*n*-butanol and *iso*-butanol) and *n*-heptane were tested in the experiments. Two port fuel injectors were mounted in the intake manifold to introduce the premixed fuels into the cylinder. Intake pressure and temperature were controlled by



external compressor and intake conditioner. The ratios between the butanol isomers and *n*-heptane could be flexibly adjusted by changing the injection duration of each injector, and thus the overall reactivity of the fuel could be well controlled. No EGR was applied in the CAT engine, and the blending ratio between butanol and *n*-heptane was changed to maintain the same CA50 timing (crank angle at which 50% accumulated heat release is reached)

between *n*-butanol and *iso*-butanol under different conditions. The indicated mean effective pressure (IMEP) was about 6.5 bar, and the pressure traces of 300 individual cycles were captured by a pressure transducer and averaged to get the averaged in-cylinder pressure. In the YC (YuChai) engine, mixtures with fixed blending ratios between the four butanol isomers and *n*-heptane (75%/25% mole fraction) were used as fuels and EGR was also

TABLE 3 | Engine specifications and HCCI operating conditions.

Engine type	CAT SCOTE	YC
Bore*stroke (mm)	137.2 × 165.1	105 × 125
Displacement (L)	2.44	1.081
Compression ratio	14.88:1	15.8:1
Chamber type	RCOI piston	Bowl in piston
Fuel injection	Port injection	Port injection
Operating conditions		
Engine (r/min)	1300	1500
IMEP (bar)	≈6.5	≈4.5
P_{in} (bar)	1.35–1.8	1.5
T_{in} (K)	313–323	343
EGR (%)	0	10–40
Phi	0.28–0.35	0.3
Fuel type	<i>n</i> -/ <i>i</i> -C ₄ H ₉ OH/ <i>n</i> -C ₇ H ₁₆	Butanol/ <i>n</i> -C ₇ H ₁₆
<i>n</i> -C ₇ H ₁₆ ratio (%)	3.3–32.8	25

applied in the experiments. Mixtures of butanol isomers and *n*-heptane were introduced through an injector mounted in the intake manifold to ensure the homogeneity of the in-cylinder mixtures. Intake pressure and temperature were also controlled by an external compressor and intake heater to maintain constant intake conditions. EGR and exhaust back pressure valves were used to adjust the EGR rate. The total fuel mass per cycle was changed to maintain a constant equivalence ratio of 0.30 under the different EGR rate conditions, resulting in an IMEP of about 4.5 bar. In this engine, a piston with CR 15.8 was used and the pressure traces of 50 individual cycles were averaged to get the averaged in-cylinder pressures. The apparent heat release rate (AHRR) was then calculated based on these experimentally measured in-cylinder pressures, and other combustion parameters, such the ignition delay and CA10 timing, could then be obtained.

The KIVA CFD code (Amsden, 1999) was used and coupled with the proposed mechanism for the HCCI engine combustion predictions. The SpeedCHEM chemistry solver was used to improve the computational efficiency (Perini et al., 2012; 2014). Homogeneous charges were assumed in the computational domain at the start of the simulation [at intake valve closing (IVC)], and the simulation ended at exhaust valve opening (EVO). Two-dimensional computational meshes for both the CAT and YC engines were used in the simulations and the geometry of the engine grids can be found in Wang et al. (2013b). The IVC temperatures in the simulations were obtained from zero-dimensional simulations and the cooling effect of the premixed fuels was also taken into consideration in the simulations.

CAT Engine HCCI Combustion

Figure 7 shows comparisons of in-cylinder pressures and AHRR between the simulations and experiments for *n*-butanol/*n*-heptane and *iso*-butanol/*n*-heptane mixtures under different intake pressure and temperature conditions on the CAT engine. It is seen that good agreements are obtained with the current mechanism. The ignition timing, pressure rise rate, in-cylinder

peak pressure, and combustion durations all agree quite well with the experimental results, which indicate that the proposed mechanism is able to capture the HCCI combustion processes of *n*-butanol and *iso*-butanol under various operating conditions.

In addition to the available HCCI experimental data for *n*-butanol and *iso*-butanol, numerical simulations were also conducted to simulate HCCI combustion processes of mixtures of *sec*-butanol/*n*-heptane and *tert*-butanol/*n*-heptane under the same conditions. The *n*-heptane blending ratios in these two mixtures were also changed to maintain similar CA50 timings compared to those of *n*-butanol and *iso*-butanol. Figure 8 shows comparisons of the *n*-heptane blending ratios and CA50 timings among the butanol isomers under the different conditions. The intake pressures and temperatures are also listed on the *x*-axis in the figures.

It is seen that the predicted CA50 timings of both *n*- and *iso*-butanol/*n*-heptane mixtures are very close to those of the experimental results. The comparison of the *n*-heptane blending ratios under the different conditions among the butanol isomers indicates that the mixture of *n*-butanol and *n*-heptane has the highest reactivity, followed by *tert*-butanol, and then *iso*-butanol and *sec*-butanol, which does not agree with the conclusions presented in Figure 2. However, this can be explained in Figure 9, which shows the ignition delays of the butanol isomer/*n*-heptane mixtures as a function of *n*-heptane blending ratio in the mixture under the 850 K, 40.0 bar, and 0.35 equivalence ratio condition, which is very close to the in-cylinder condition prior to ignition for the 1.35 bar intake pressure and 323 K intake temperature condition in the CAT HCCI experiments. It is seen that the reactivity of the *tert*-butanol/*n*-heptane mixture is higher than the *n*-butanol/*n*-heptane mixture only if the *n*-heptane blending ratio is higher than 20% in the mixture. This is reasonable since no matter how difficult the H atom abstraction reaction is with *tert*-butanol, the presence of *n*-heptane still dominates the overall reactivity. Thus, even if there is no OH radical absorption from butanol in the mixture, due to the much lower reactivity of neat *tert*-butanol, the reactivity enhanced by the OH radicals that are released from *tert*-butanol H atom abstraction reactions still cannot compensate for the low reactivity of *tert*-butanol itself. The following HCCI experiments on the YC engine also justify this point.

YC Engine HCCI Combustion

Figure 10 shows comparisons of in-cylinder pressures and AHRRs for all the butanol isomer/*n*-heptane mixtures under different EGR rate conditions on the YC engine. Again, it is seen that the present mechanism is able to accurately capture the HCCI combustion processes of all the fuels under different operating conditions. Since one of the major targets for the development of a reduced mechanism is to capture the combustion process in real combustion devices, the current results suggest that the performance of the mechanism is reliable, at least under pure chemical kinetically controlled lean HCCI conditions.

Figure 11 shows comparisons of in-cylinder pressures between the experiments and simulations for the tested mixtures at 20% EGR rate condition. As already shown in Figure 3, the reactivity

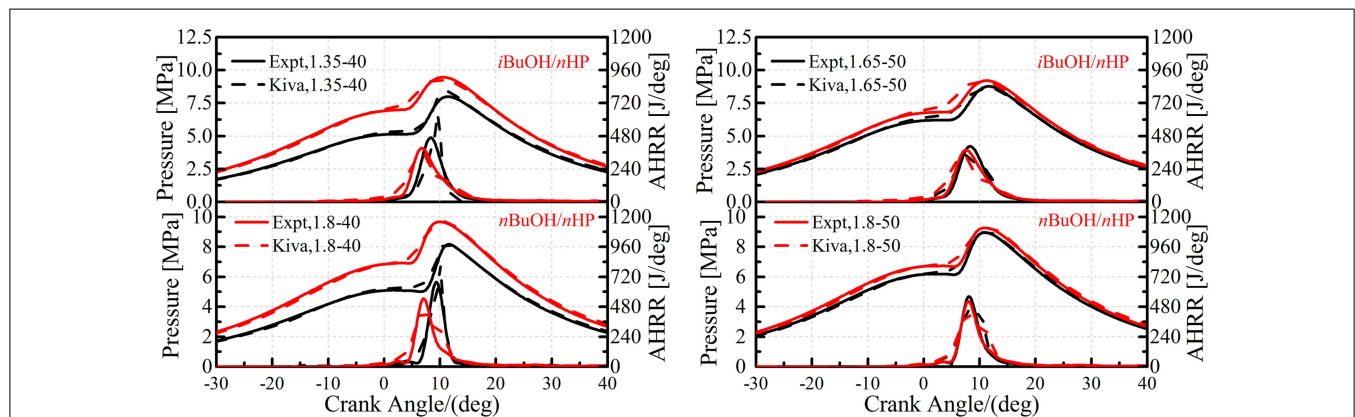


FIGURE 7 | Comparisons of in-cylinder pressure and AHRR between simulations and experiments in the CAT engine.

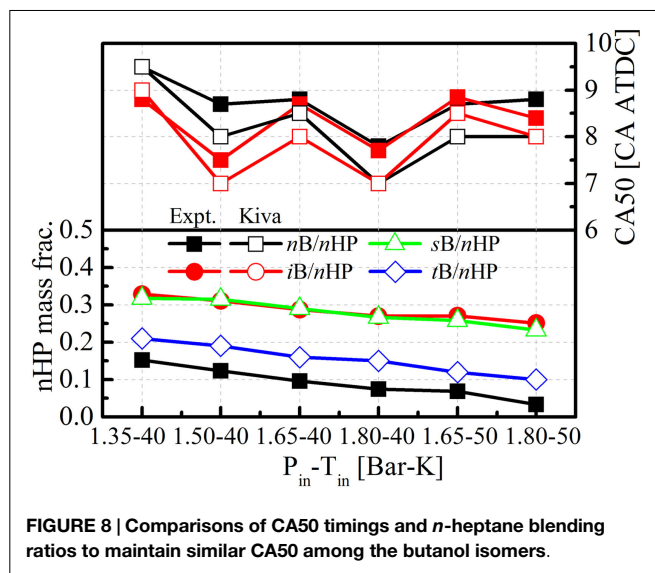


FIGURE 8 | Comparisons of CA50 timings and *n*-heptane blending ratios to maintain similar CA50 among the butanol isomers.

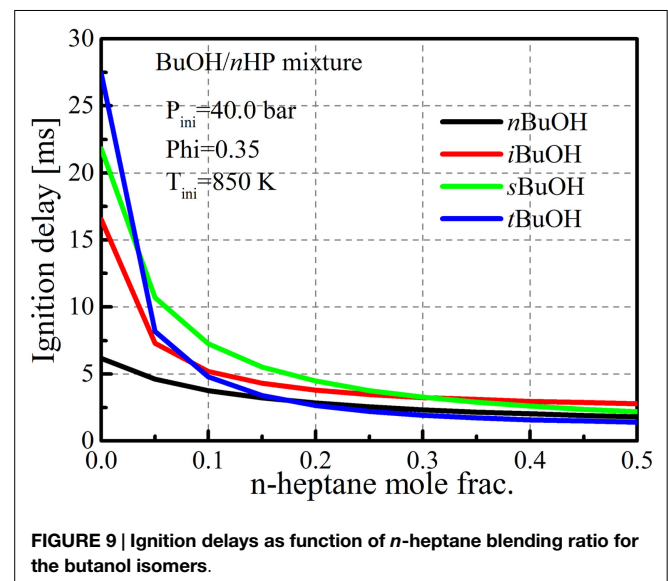


FIGURE 9 | Ignition delays as function of *n*-heptane blending ratio for the butanol isomers.

of the *tert*-butanol/*n*-heptane mixture is the highest among the four butanol isomers once the *n*-heptane blending ratio exceeds 20%. The current HCCI combustion data also show a similar trend, the *tert*-butanol/*n*-heptane mixture (75%/25% in mole) shows the shortest ignition delay, followed by *n*-butanol and then *iso*-butanol and *sec*-butanol. The reasons for those results were explained in the mechanism adjustment section, namely both the fuel + OH and fuel + CH₃O₂ reactions are responsible for the higher reactivity of *tert*-butanol/*n*-heptane mixtures. The simulations also capture this trend, which again confirms the reliability of the proposed mechanism.

Figure 12 shows comparisons of the CA50 timings between experiments and simulations under different EGR rate conditions. It is clearly seen that the simulations capture the experimental trends. The relative reactivity among the butanol isomers and *n*-heptane is well reproduced by the simulations. Mixtures of *tert*-butanol and *n*-heptane show the earliest CA50 timing, followed by *n*-butanol and then *iso*-butanol and *sec*-butanol. For *n*-butanol, *sec*-butanol, and *iso*-butanol, the CA50 timing agrees with their

RON trends, namely that *n*-butanol has the lowest RON while *iso*-butanol has the highest. Combined with the previous works conducted for PRF, methanol, and ethanol HCCI combustion, it is therefore concluded that the current reduced mechanism can be used for engine combustion simulations with alcohols.

Conclusion

In the current study, a reduced PRF-Alcohol-DTBP mechanism with 108 species and 435 reactions has been proposed for HCCI combustion simulations. The proposed mechanism is formulated based on a base-reduced PRF mechanism, and the detailed butanol mechanisms developed by Sarathy et al. (2012) were reduced and incorporated into the base mechanism. The model can predict the ignition and combustion processes of PRF, methanol, ethanol, DTBP, and the four butanol isomers. Experimental HCCI combustion results for butanol isomer/*n*-heptane mixtures were also obtained from two different diesel engines to

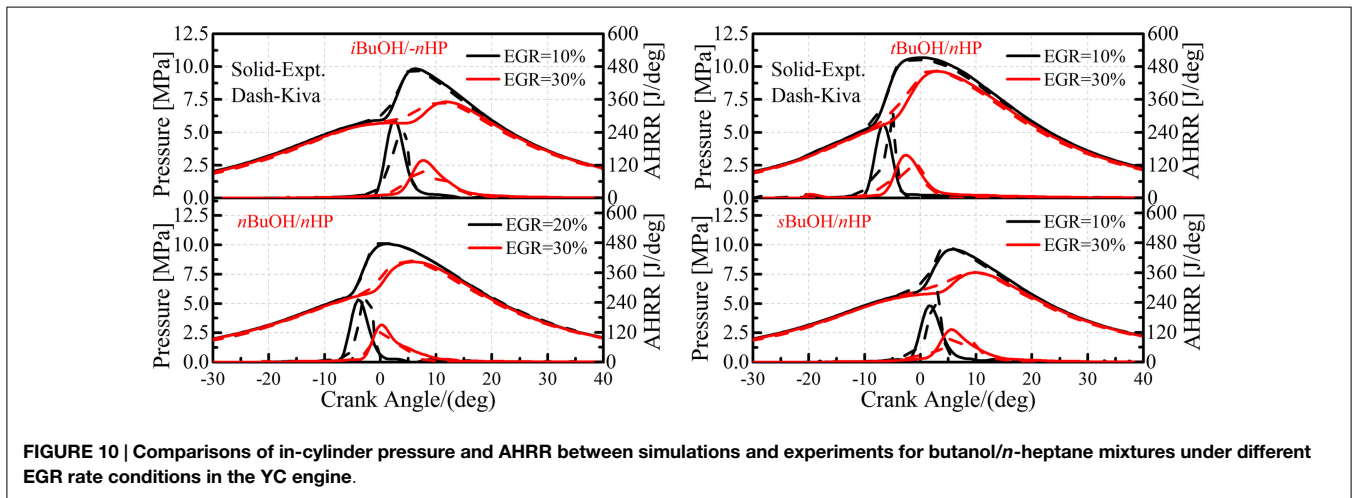


FIGURE 10 | Comparisons of in-cylinder pressure and AHRR between simulations and experiments for butanol/*n*-heptane mixtures under different EGR rate conditions in the YC engine.

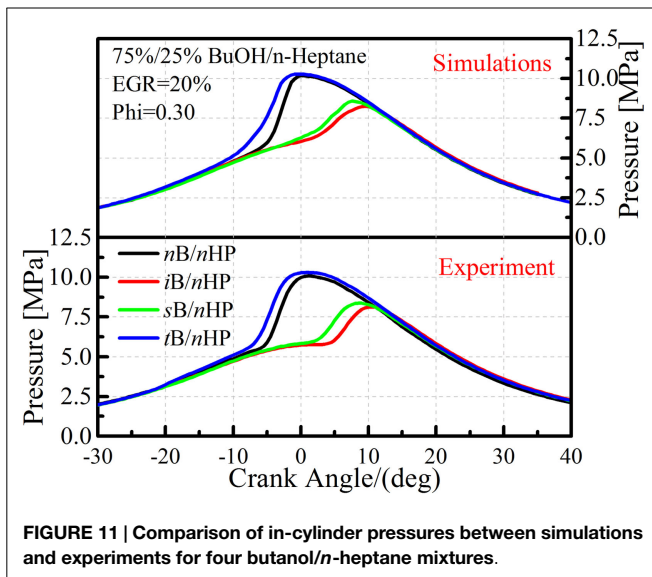


FIGURE 11 | Comparison of in-cylinder pressures between simulations and experiments for four butanol/*n*-heptane mixtures.

validate the mechanisms. The major conclusions can be summarized as follows:

1. An integrated PRF–methanol–ethanol–butanol–DTBP kinetic mechanism with 108 species and 435 reactions has been developed for HCCI combustion simulations. The proposed mechanism has been validated with various experimental data, including shock tube ignition delays, laminar flame speeds, species profiles from premixed flames, and also HCCI engine combustion data, and yields good agreements for a wide range of validation conditions.
2. Kinetic analysis shows that, although the reactivity of neat *tert*-butanol is the lowest, mixtures of *tert*-butanol/*n*-heptane exhibit the highest reactivity among mixtures of the butanol isomers and *n*-heptane if the *n*-heptane blending ratio exceeds about 20%.
3. It is found that the highest C–H bond energy in the *tert*-butanol molecule is partially responsible for this result. The high C–H bond energy reduces the OH radical absorption

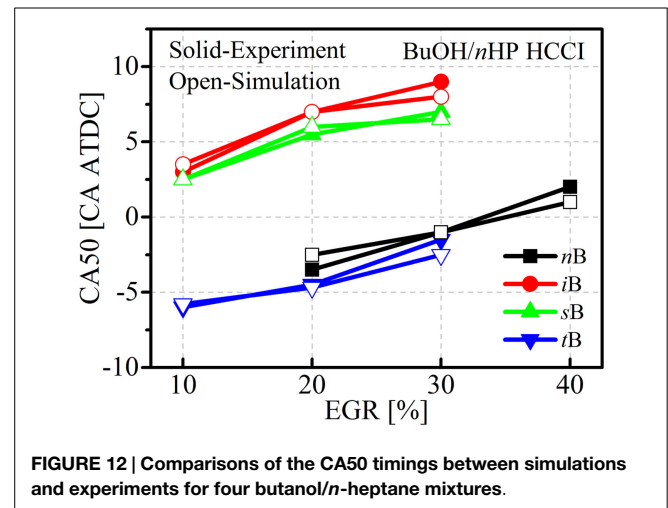


FIGURE 12 | Comparisons of the CA50 timings between simulations and experiments for four butanol/*n*-heptane mixtures.

ability of *tert*-butanol, which results in more available OH radicals in the system to promote ignition.

4. In addition to the bond energy effect, it was found that the reaction $tC_4H_9OH + CH_3O_2 \rightleftharpoons tC_4H_9O + CH_3O_2H$ also plays an important role during this process. The tC_4H_9O radical is also the major intermediate species in DTBP oxidation, which produces CH_3O_2 and CH_3O_2H , and eventually the OH radical is generated through this pathway.
5. HCCI combustion data from two different diesel engines for butanol isomer/*n*-heptane mixtures were used to validate the proposed mechanism. The chemical kinetic mechanisms are able to capture HCCI combustion processes of various butanol/*n*-heptane mixtures over a range of operating conditions. In addition, the HCCI experiments also show that mixtures of *tert*-butanol/*n*-heptane have the highest reactivity among the tested fuels, which is in agreement with Haas et al.'s results (Haas et al., 2011), and the present simulations also capture this trend.
6. The overall results indicate that the current mechanisms can be used for HCCI engine combustion predictions of PRF and alcohol fuels. However, further improvements can still be made

when more validation data become available, especially ignition delay data under low-temperature conditions.

Acknowledgments

The authors acknowledge financial support provided by the Princeton Combustion Energy Frontier Research Center. The authors are also thankful for support from Reaction Design for

providing access to the CHEMKIN Pro software for the chemistry simulations.

Supplementary Material

The mechanism developed in the current study is provided as supplementary material at <http://journal.frontiersin.org/article/10.3389/fmech.2015.00003/abstract>.

References

- Agarwal, A. K. (2007). Biofuels (alcohols and biodiesel) applications as fuels for internal combustion engines. *Prog. Energy Combust. Sci.* 33, 233–271. doi:10.1016/j.peccs.2006.08.003
- Ajav, E. A., Singh, B., and Bhattacharya, T. K. (1999). Experimental study of some performance parameters of a constant speed stationary diesel engine using ethanol-diesel blends as fuel. *Biomass Bioenergy* 17, 357–365. doi:10.1016/S0961-9534(99)00048-3
- Amsden, A. (1999). *Kiva-3v, Release 2, Improvements to Kiva-3v*. Report LA-13608-MS, LA-UR-99-915. Los Alamos, NM: Los Alamos National Laboratory.
- Aranda, V., Christensen, J. M., Alzueta, M. U., Glarborg, P., Gersen, S., Gao, Y., et al. (2013). Experimental and kinetic modeling study of methanol ignition and oxidation at high pressure. *Int. J. Chem. Kinet.* 45, 283–294. doi:10.1002/kin.20764
- Balki, M. K., Sayin, C., and Canakci, M. (2014). The effect of different alcohol fuels on the performance, emission and combustion characteristics of a gasoline engine. *Fuel* 115, 901–906. doi:10.1016/j.fuel.2012.09.020
- Bec, I. L. R., Zhu, Y., Davidson, D. F., and Hanson, R. K. (2014). Shock tube measurements of ignition delay times for the butanol isomers using the constrained-reaction-volume strategy. *Int. J. Chem. Kinet.* 46, 433–442. doi:10.1002/kin.20859
- Beckmann, J., Cai, L., and Pitsch, H. (2014). Experimental investigation of the laminar burning velocities of methanol, ethanol, n-propanol, and n-butanol at high pressure. *Fuel* 117(Part A), 340–350. doi:10.1016/j.fuel.2013.09.025
- Black, G., Curran, H. J., Pichon, S., Simmie, J. M., and Zhukov, V. (2010). Bio-butanol: combustion properties and detailed chemical kinetic model. *Combust. Flame* 157, 363–373. doi:10.1016/j.combustflame.2009.07.007
- Canakci, M., Ozsezen, A. N., Alptekin, E., and Eyidogan, M. (2013). Impact of alcohol-gasoline fuel blends on the exhaust emission of an SI engine. *Renew. Energy* 52, 111–117. doi:10.1016/j.renene.2012.09.062
- Chen, Z., Wu, Z., Liu, J., and Lee, C. (2014). Combustion and emissions characteristics of high n-butanol/diesel ratio blend in a heavy-duty diesel engine and EGR impact. *Energy Convers. Manag.* 78, 787–795. doi:10.1016/j.enconman.2013.11.037
- Dagaut, P., Sarathy, S. M., and Thomson, M. J. (2009). A chemical kinetic study of n-butanol oxidation at elevated pressure in a jet stirred reactor. *Proc. Combust. Inst.* 32, 229–237. doi:10.1016/j.proci.2008.05.005
- Dagaut, P., and Togbe, C. (2009). Experimental and modeling study of the kinetics of oxidation of butanol n-heptane mixtures in a jet-stirred reactor. *Energy. Fuel* 23, 3527–3535. doi:10.1021/e900261f
- Dagaut, P., and Togbé, C. (2010). Experimental and modeling study of the kinetics of oxidation of ethanol-n-heptane mixtures in a jet-stirred reactor. *Fuel* 89, 280–286. doi:10.1016/j.fuel.2009.06.035
- Dayma, G., Ali, K. H., and Dagaut, P. (2007). Experimental and detailed kinetic modeling study of the high pressure oxidation of methanol sensitized by nitric oxide and nitrogen dioxide. *Proc. Combust. Inst.* 31, 411–418. doi:10.1016/j.proci.2006.07.143
- Dempsey, A. B., Walker, N. R., and Reitz, R. (2013). Effect of cetane improvers on gasoline, ethanol, and methanol reactivity and the implications for RCCI combustion. *SAE Int. J. Fuels Lubr.* 6, 170–187. doi:10.4271/2013-01-1678
- Elik, M. B., Zdaljan, B., and Alkan, F. (2011). The use of pure methanol as fuel at high compression ratio in a single cylinder gasoline engine. *Fuel* 90, 1591–1598. doi:10.1016/j.fuel.2010.10.035
- Engine Research Center. (2013). Engine Research Center, University of Wisconsin-Madison. Available at: <http://www.erc.wisc.edu/chemicalreaction.php>
- Esarte, C., Abián, M., Millera, A., Bilbao, R., and Alzueta, M. U. (2012). Gas and soot products formed in the pyrolysis of acetylene mixed with methanol, ethanol, isopropanol or n-butanol. *Energy* 43, 37–46. doi:10.1016/j.energy.2011.11.027
- Gu, X., Huang, Z., Cai, J., Gong, J., Wu, X., and Lee, C.-F. (2012). Emission characteristics of a spark-ignition engine fuelled with gasoline-n-butanol blends in combination with EGR. *Fuel* 93, 611–617. doi:10.1016/j.fuel.2011.11.040
- Haas, F. M., Ramcharan, A., and Dryer, F. L. (2011). Relative reactivities of the isomeric butanols and ethanol in an ignition quality tester. *Energy. Fuel* 25, 3909–3916. doi:10.1021/ef2008024
- Harper, M. R., Van Geem, K. M., Pyl, S. P., Marin, G. B., and Green, W. H. (2011). Comprehensive reaction mechanism for n-butanol pyrolysis and combustion. *Combust. Flame* 158, 16–41. doi:10.1016/j.combustflame.2010.06.002
- Heufer, K. A., Fernandes, R. X., Olivier, H., Beekmann, J., Röhl, O., and Peters, N. (2011). Shock tube investigations of ignition delays of n-butanol at elevated pressures between 770 and 1250 kPa. *Proc. Combust. Inst.* 33, 359–366. doi:10.1016/j.proci.2010.06.052
- Heufer, K. A., and Olivier, H. (2010). Determination of ignition delay times of different hydrocarbons in a new high pressure shock tube. *Shock Waves* 20, 307–316. doi:10.1007/s00193-010-0262-2
- Hudzik, J. M., Bozzelli, J. W., and Simmie, J. M. (2014). Thermochemistry of C7H16 to C10H22 alkane isomers: primary, secondary, and tertiary C–H bond dissociation energies and effects of branching. *J. Phys. Chem. A* 118, 9364–9379. doi:10.1021/jp503587b
- Jin, C., Yao, M., Liu, H., Lee, C.-F. F., and Ji, J. (2011). Progress in the production and application of n-butanol as a biofuel. *Renew. Sustain. Energy Rev.* 15, 4080–4106. doi:10.1016/j.rser.2011.06.001
- Karwat, D. M. A., Wagnon, S. W., Wooldridge, M. S., and Westbrook, C. K. (2012). On the combustion chemistry of n-heptane and n-butanol blends. *J. Phys. Chem. A* 116, 12406–12421. doi:10.1021/jp309358h
- Kumar, K., and Sung, C.-J. (2011). Autoignition of methanol: experiments and computations. *Int. J. Chem. Kinet.* 43, 175–184. doi:10.1002/kin.20546
- Leplat, N., Dagaut, P., Togbé, C., and Vandooren, J. (2011). Numerical and experimental study of ethanol combustion and oxidation in laminar premixed flames and in jet-stirred reactor. *Combust. Flame* 158, 705–725. doi:10.1016/j.combustflame.2010.12.008
- Li, J., Zhao, Z., Kazakov, A., Chaos, M., Dryer, F. L., and Scire, J. J. (2007). A comprehensive kinetic mechanism for CO, CH₂O, and CH₃OH combustion. *Int. J. Chem. Kinet.* 39, 109–136. doi:10.1002/kin.20218
- Liu, H., Wang, X., Zheng, Z., Gu, J., Wang, H., and Yao, M. (2014). Experimental and simulation investigation of the combustion characteristics and emissions using n-butanol/biodiesel dual-fuel injection on a diesel engine. *Energy* 74, 741–752. doi:10.1016/j.energy.2014.07.041
- Liu, W., Kelley, A. P., and Law, C. K. (2011). Non-premixed ignition, laminar flame propagation, and mechanism reduction of n-butanol, iso-butanol, and methyl butanoate. *Proc. Combust. Inst.* 33, 995–1002. doi:10.1016/j.proci.2010.05.084
- Marinov, N. M. (1999). A detailed chemical kinetic model for high temperature ethanol oxidation. *Int. J. Chem. Kinet.* 31, 183–220. doi:10.1002/(SICI)1097-4601(1999)31:3<183::AID-KIN3>3.0.CO;2-X
- Metcalfe, W. K., Burke, S. M., Ahmed, S. S., and Curran, H. J. (2013). A hierarchical and comparative kinetic modeling study of C1 - C2 hydrocarbon and oxygenated fuels. *Int. J. Chem. Kinet.* 45, 638–675. doi:10.1002/kin.20802
- Moss, J. T., Berkowitz, A. M., Oehlschlaeger, M. A., Biet, J., Warth, V. R., Glaude, P.-A., et al. (2008). An experimental and kinetic modeling study of the oxidation of the four isomers of butanol. *J. Phys. Chem. A* 112, 10843–10855. doi:10.1021/jp806464p

- Noorani, K. E., Akih-Kumgeh, B., and Bergthorson, J. M. (2010). Comparative high temperature shock tube ignition of C1-C4 primary alcohols. *Energ. Fuel* 24, 5834–5843. doi:10.1021/ef1009692
- Norton, T. S., and Dryer, F. L. (1991). The flow reactor oxidation of C1-C4 alcohols and MTBE. *Symp. Combust. Proc.* 23, 179–185. doi:10.1016/S0082-0784(06)80257-2
- Oßwald, P., Gülkenberg, H., Kohse-Höinghaus, K., Yang, B., Yuan, T., and Qi, F. (2011). Combustion of butanol isomers-A detailed molecular beam mass spectrometry investigation of their flame chemistry. *Combust. Flame* 158, 2–15. doi:10.1016/j.combustflame.2010.06.003
- Pan, L., Zhang, Y., Tian, Z., Yang, F., and Huang, Z. (2014). Experimental and kinetic study on ignition delay times of iso-butanol. *Energ. Fuel* 28, 2160–2169. doi:10.1021/jp806464p
- Pepiot-Desjardins, P., and Pitsch, H. (2008). An efficient error-propagation-based reduction method for large chemical kinetic mechanisms. *Combust. Flame* 154, 67–81. doi:10.1021/ar300359w
- Perini, F., Galligani, E., and Reitz, R. D. (2012). An analytical Jacobian approach to sparse reaction kinetics for computationally efficient combustion modeling with large reaction mechanisms. *Energ. Fuel* 26, 4804–4822. doi:10.1021/ef300747n
- Perini, F., Galligani, E., and Reitz, R. D. (2014). A study of direct and Krylov iterative sparse solver techniques to approach linear scaling of the integration of chemical kinetics with detailed combustion mechanisms. *Combust. Flame* 161, 1180–1195. doi:10.1016/j.combustflame.2013.11.017
- Rakopoulos, D. C., Rakopoulos, C. D., Hountalas, D. T., Kakaras, E. C., Giakoumis, E. G., and Papagiannakis, R. G. (2010). Investigation of the performance and emissions of bus engine operating on butanol/diesel fuel blends. *Fuel* 89, 2781–2790. doi:10.1016/j.fuel.2010.03.047
- Rakopoulos, D. C., Rakopoulos, C. D., Kakaras, E. C., and Giakoumis, E. G. (2008). Effects of ethanol-diesel fuel blends on the performance and exhaust emissions of heavy duty DI diesel engine. *Energ. Convers. Manag.* 49, 3155–3162. doi:10.1016/j.enconman.2008.05.023
- Reaction Design. (2008). CHEMKIN PRO: a chemical kinetics package for the analysis of gas-phase chemical kinetics. *React. Des.*
- Sarathy, S. M., Oßwald, P., Hansen, N., and Kohse-Höinghaus, K. (2014). Alcohol combustion chemistry. *Prog. Energy Combust. Sci.* 44, 40–102. doi:10.1016/j.pecc.2014.04.003
- Sarathy, S. M., Thomson, M. J., Togbé, C., Dagaut, P., Halter, F., and Mounaim-Rousselle, C. (2009). An experimental and kinetic modeling study of n-butanol combustion. *Combust. Flame* 156, 852–864. doi:10.1039/c1cp21663e
- Sarathy, S. M., Vranckx, S., Yasunaga, K., Mehl, M., Oßwald, P., Metcalfe, W. K., et al. (2012). A comprehensive chemical kinetic combustion model for the four butanol isomers. *Combust. Flame* 159, 2028–2055. doi:10.1016/j.combustflame.2011.12.017
- Shi, Y., Ge, H.-W., Brakora, J. L., and Reitz, R. D. (2010). Automatic chemistry mechanism reduction of hydrocarbon fuels for HCCI engines based on DRGEP and PCA methods with error control. *Energ. Fuel* 24, 1646–1654. doi:10.1021/ef901469p
- Shi, Y., Green, W. H. Jr., Wong, H.-W., and Oluwole, O. O. (2011). Redesigning combustion modeling algorithms for the graphics processing unit (GPU): chemical kinetic rate evaluation and ordinary differential equation integration. *Combust. Flame* 158, 836–847. doi:10.1016/j.combustflame.2011.01.024
- Stranic, I., Chase, D. P., Harmon, J. T., Yang, S., Davidson, D. F., and Hanson, R. K. (2012). Shock tube measurements of ignition delay times for the butanol isomers. *Combust. Flame* 159, 516–527. doi:10.1021/jp806464p
- Togbé, C., Mzè-Ahmed, A., and Dagaut, P. (2010). Kinetics of oxidation of 2-butanol and isobutanol in a jet-stirred reactor: experimental study and modeling investigation. *Energ. Fuel* 24, 5244–5256. doi:10.1021/ef1008488
- Veloo, P. S., and Egolfopoulos, F. N. (2011). Flame propagation of butanol isomers/air mixtures. *Proc. Combust. Inst.* 33, 987–993. doi:10.1016/j.proci.2010.06.163
- Veloo, P. S., Wang, Y. L., Egolfopoulos, F. N., and Westbrook, C. K. (2010). A comparative experimental and computational study of methanol, ethanol, and n-butanol flames. *Combust. Flame* 157, 1989–2004. doi:10.1016/j.combustflame.2010.04.001
- Vranckx, S., Heufer, K. A., Lee, C., Olivier, H., Schill, L., Kopp, W. A., et al. (2011). Role of peroxy chemistry in the high-pressure ignition of n-butanol Experiments and detailed kinetic modelling. *Combust. Flame* 158, 1444–1455. doi:10.1016/j.combustflame.2010.12.028
- Wang, H., Dempsey, A. B., Yao, M., Jia, M., and Reitz, R. D. (2014a). Kinetic and numerical study on the effects of di-tert-butyl peroxide additive on the reactivity of methanol and ethanol. *Energ. Fuel* 28, 5480–5488. doi:10.1021/ef500867p
- Wang, H., Zheng, Z., Yao, M., and Reitz, R. D. (2014b). An experimental and numerical study on the effects of fuel properties on the combustion and emissions of low-temperature combustion diesel engines. *Combust. Sci. Technol.* 186, 1795–1815. doi:10.1080/00102202.2014.920836
- Wang, H., Reitz, R. D., Yao, M., Yang, B., Jiao, Q., and Qiu, L. (2013a). Development of an n-heptane-n-butanol-PAH mechanism and its application for combustion and soot prediction. *Combust. Flame* 160, 504–519. doi:10.1016/j.combustflame.2012.11.017
- Wang, H., Yao, M., and Reitz, R. D. (2013b). Development of a reduced primary reference fuel mechanism for internal combustion engine combustion simulations. *Energ. Fuel* 27, 7843–7853. doi:10.1021/ef401992e
- Weber, B. W., and Sung, C.-J. (2013). Comparative autoignition trends in butanol isomers at elevated pressure. *Energ. Fuel* 27, 1688–1698. doi:10.1021/ef302195c
- Welz, O., Savee, J. D., Eskola, A. J., Sheps, L., Osborn, D. L., and Taatjes, C. A. (2013). Low-temperature combustion chemistry of biofuels: pathways in the low-temperature (550–700K) oxidation chemistry of isobutanol and tert-butanol. *Proc. Combust. Inst.* 34, 493–500. doi:10.1039/c2cp23248k
- Wu, F., and Law, C. K. (2013). An experimental and mechanistic study on the laminar flame speed, Markstein length and flame chemistry of the butanol isomers. *Combust. Flame* 160, 2744–2756. doi:10.1016/j.combustflame.2013.06.015
- Xu, H., Yao, C., Yuan, T., Zhang, K., and Guo, H. (2011). Measurements and modeling study of intermediates in ethanol and dimethyl ether low-pressure premixed flames using synchrotron photoionization. *Combust. Flame* 158, 1673–1681. doi:10.1016/j.combustflame.2011.01.004
- Yang, Z., Qian, Y., Yang, X., Wang, Y., Wang, Y., Huang, Z., et al. (2013). Autoignition of n-butanol/n-heptane blend fuels in a rapid compression machine under low-to-medium temperature ranges. *Energ. Fuel* 27, 7800–7808. doi:10.1021/ef401774f
- Yao, M., Wang, H., Zheng, Z., and Yue, Y. (2010). Experimental study of n-butanol additive and multi-injection on HD diesel engine performance and emissions. *Fuel* 89, 2191–2201. doi:10.1016/j.fuel.2010.04.008
- Zhang, J., Niu, S., Zhang, Y., Tang, C., Jiang, X., Hu, E., et al. (2013). Experimental and modeling study of the auto-ignition of n-heptane/n-butanol mixtures. *Combust. Flame* 160, 31–39. doi:10.1016/j.combustflame.2012.09.006
- Zhang, Z., Huang, Z., Wang, X., Xiang, J., Wang, X., and Miao, H. (2008). Measurements of laminar burning velocities and Markstein lengths for methanol-air-nitrogen mixtures at elevated pressures and temperatures. *Combust. Flame* 155, 358–368. doi:10.1016/j.combustflame.2008.07.005
- Zheng, Z., Li, C., Liu, H., Zhang, Y., Zhong, X., and Yao, M. (2015). Experimental study on diesel conventional and low temperature combustion by fueling four isomers of butanol. *Fuel* 141, 109–119. doi:10.1016/j.fuel.2014.10.053
- Zhu, Y., Davidson, D. F., and Hanson, R. K. (2013). 1-Butanol ignition delay times at low temperatures: an application of the constrained-reaction-volume strategy. *Combust. Flame* 161, 634–643. doi:10.1016/j.combustflame.2013.06.028

Conflict of Interest Statement: The authors declare that the research was conducted in the absence of any commercial or financial relationships that could be construed as a potential conflict of interest.

Copyright © 2015 Wang, DelVescovo, Zheng, Yao and Reitz. This is an open-access article distributed under the terms of the Creative Commons Attribution License (CC BY). The use, distribution or reproduction in other forums is permitted, provided the original author(s) or licensor are credited and that the original publication in this journal is cited, in accordance with accepted academic practice. No use, distribution or reproduction is permitted which does not comply with these terms.